Climatic Change (2007) 81:53–70
DOI 10.1007/s10584-006-9228-x

An intercomparison of regional climate simulations for Europe: assessing uncertainties in model projections

M. Déqué · D. P. Rowell · D. Lüthi · F. Giorgi · J. H. Christensen · B. Rockel · D. Jacob · E. Kjellström · M. de Castro · B. van den Hurk

Received: 15 February 2005 / Accepted: 17 October 2006 / Published online: 20 March 2007

M. Déqué (✉)
Météo-France, Centre National de Recherches Météorologiques, 42 Avenue Coriolis,
31057 Toulouse Cedex 01, France
e-mail: Michel.Deque@meteo.fr

D. P. Rowell
Met Office, Hadley Centre for Climate Prediction and Research, FitzRoy Road, Exeter,
Devon EX1 3PB, UK

D. Lüthi
Swiss Federal Institute of Technology, Institute for Atmospheric and Climate Science, ETH,
Winterthurerstrasse 190, 8057 Zürich, Switzerland

F. Giorgi
Abdus Salam International Centre for Theoretical Physics, Trieste, Italy

J. H. Christensen
Danish Meteorological Institute, Lyngbyvej 100, 2100 Copenhagen Ø, Denmark

B. Rockel
GKSS Forschungszentrum Geesthacht GmbH, Institute of Coastal Research, Max Planck Strasse,
21502 Geesthacht, Germany

D. Jacob
Max-Planck-Institut für Meteorologie, Bundesstrasse 55, 20146 Hamburg, Germany

E. Kjellström
Swedish Meteorological and Hydrological Institute, Folkborgsvägen 1, 60176 Norrköping, Sweden

M. de Castro
Dept. de Ciencias Ambientales, Universidad de Castilla La Mancha, Campus Tecnologico,
45071 Toledo, Spain

B. van den Hurk
KNMI, Postbus 201, 3730 AE De Bilt, The Netherlands

Abstract Ten regional climate models (RCM) have been integrated with the standard forcings of the PRUDENCE experiment: IPCC-SRES A2 radiative forcing and Hadley Centre boundary conditions. The response over Europe, calculated as the difference between the 2071–2100 and the 1961–1990 means can be viewed as an expected value about which various uncertainties exist. Uncertainties are measured here by variance in eight sub-European boxes. Four sources of uncertainty can be evaluated with the material provided by the PRUDENCE project. Sampling uncertainty is due to the fact that the model climate is estimated as an average over a finite number of years (30). Model uncertainty is due to the fact that the models use different techniques to discretize the equations and to represent sub-grid effects. Radiative uncertainty is due to the fact that IPCC-SRES A2 is merely one hypothesis. Some RCMs have been run with another scenario of greenhouse gas concentration (IPCC-SRES B2). Boundary uncertainty is due to the fact that the regional models have been run under the constraint of the same global model. Some RCMs have been run with other boundary forcings. The contribution of the different sources varies according to the field, the region and the season, but the role of boundary forcing is generally greater than the role of the RCM, in particular for temperature. Maps of minimum expected 2m temperature and precipitation responses for the IPCC-A2 scenario show that, despite the above mentioned uncertainties, the signal from the PRUDENCE ensemble is significant.

1 Introduction

Our source of information about past climate changes comes from observation. The information about possible future climate changes is obtained through numerical climate models (IPCC 2001). Different models behave differently and there is no established way to tell which model represents the most probable version of the future. Evaluating the uncertainty is thus as important as averaging the different possible scenarios to get the best estimate. Uncertainty can be evaluated by performing several simulations with the same model (e.g. Giorgi and Francisco 2000). Using different climate models with the same forcing is another method of uncertainty evaluation (e.g. Crossley et al. 2000). The two approaches can be combined as in Räisänen et al. (2004).

Uncertainties in projected climate change arise from various sources. The amplitude of anthropogenic emissions and the resulting greenhouse gas (GHG) concentration is the initial source in the causal chain. The formulation and accuracy of the atmosphere–ocean general circulation model (AOGCM) driven by this radiative forcing causes an additional level of uncertainty. Furthermore, in order to provide detailed projections of local climate change to the impacts community and policy makers, a further tier of complexity is required. This is the forcing of a high resolution regional climate model (RCM) by the AOGCM. This introduces a third source of uncertainty. Finally, the simulated, as well as the actual, climate exhibits interannual variability due to the chaotic nature of atmosphere and ocean behavior. As the climate statistics are estimated from a finite sample, a fourth source of uncertainty is introduced by this sampling.

The EC-funded project Prediction of Regional scenario and Uncertainties for Defining EuropeaN Climate change risks and Effects project (PRUDENCE, Christensen et al. 2002) is a good opportunity to investigate the relative contributions of the above mentioned uncertainty sources. Rowell (2006) examines the variance in subsamples of the PRUDENCE standard database over the British Isles. His main conclusion is that the uncertainty in GCM formulation plays the major role. The aim of this paper is to generalize the results to all European sub-regions and use variance analysis tools to improve the comparison of the partial variances by using as many model runs as possible. This requires data reconstruction. Indeed

the PRUDENCE database does not offer all combinations of GHG concentration scenarios, GCMs and RCMs. Amongst the many fields archived in the PRUDENCE database, we consider here as in Rowell (2006) 2m temperature and precipitation.

The word "uncertainty" may get different meanings in the climate change literature. In the present paper, uncertainty means spread: when we are faced with a choice with several options, taking a particular one, or the average of the available ones, generates some uncertainty which is traditionally measured by standard deviation. This meaning is different from the meaning in prediction science, where uncertainty measures a distance between the actual value to be predicted and its prediction; this uncertainty is traditionally evaluated by rms error in past forecasts.

In Section 2, we present the 10 RCMs and the experiments used in the study. In Section 3, the variance of all climate changes available is partitioned using statistical techniques. Section 4 is restricted to the modeling uncertainty: using IPCC-SRES A2 scenario and neglecting sampling uncertainty, a confidence interval is calculated for the PRUDENCE mean climate change response, using two different approaches. Conclusions and perspectives are given in Section 5.

2 Models and experiments available

2.1 Regional climate models

In PRUDENCE, ten RCMs with resolution of about 50 km over Europe have been used to simulate the years 1961–1990 (reference) and 2071–2100 (climate change).

1. Danish Meteorological Institute (DMI) uses HIRHAM. HIRHAM was first developed by Christensen and van Meijgaard (1992) and later updated by Christensen et al. (1996). Further updates utilizing new high resolution physiographical data sets of surface topography and land use classification have also been introduced (Hagemann et al. 1999; Christensen et al. 2001). Aspects of the models ability to simulate present day and future climate are described in Christensen et al. (1998) and Christensen and Christensen (2003; 2004).
2. The Hadley Centre (HC) uses HadRM3H (Hudson and Jones 2002b). The configuration of the model is very similar to that of HadRM3P which was developed, along with its parent GCM HadAM3P (Jones et al. 2005), to provide realistic simulation of regional climate globally. The main changes are related to calculation of large-scale cloud and assumptions about the radiative effects of convective clouds. Consequent changes were made to parameters in the precipitation scheme relating to precipitation efficiency to ensure reasonable vertical cloud profiles, cloud forcing and radiation fields.
3. Eidgenössische Technische Hochschule Zürich (ETHZ) uses the CHRM. The most recent description of the model is contained in Vidale et al. (2003). The model has been tested regarding its ability to represent the continental and Alpine-scale water cycle (e.g. Frei et al. 2003), and has been used for a wide range of process studies (Schär et al. 1999; Heck et al. 2001) and climate change studies (Schär et al. 2004).
4. Geesthacht Institute for Coastal Research (GKSS) uses CLM. The Climate version of the Lokal Modell (LM) is a non-hydrostatic regional climate model. It has the same dynamic and physical core as the weather forecast model LM of the German Weather Service (DWD). A detailed description of the LM is given by Steppeler et al. (2003).

5. Max Planck Institute (MPI) uses REMO (Jacob 2001). REMO is based on the EM/DM model of the German Weather Service as CHRM is and it uses slightly modified physical parameterization schemes taken from ECHAM4 as HIRHAM does. It has been tested in different climates (Semmler et al. 2004; Aldrian et al. 2004) and the focus for validation lies on the hydrological cycle, e.g. Frei et al. (2003), Hennemuth et al. (2003) and Lehmann et al. (2004).
6. Swedish Meteorological and Hydrological Institute (SMHI) uses the Rossby Centre 6. Atmosphere Ocean model (RCAO). RCAO consists of an atmospheric part RCA2 (Jones et al. 2004) and an ocean model RCO (Meier et al. 2003). The coupling of the model components is described in Döscher et al. (2002) and the results from the simulations used here are described in Räisänen et al. (2004).
7. Universidad Complutense de Madrid (UCM) uses PROMES. First version of this model was originally developed by Castro et al. (1993) and its current complete version was used in various climate experiments (e.g. Gallardo et al. 2001; Gaertner et al. 2001; Arribas et al. 2003). Partial results from the control and scenario simulations within PRUDENCE project are described in Sanchez et al. (2004).
8. International Center for Theoretical Physics (ICTP) uses RegCM. This model was originally developed by Giorgi et al. (1993a,b) and then augmented as described by Giorgi et al. (1999) and Pal et al. (2000). The results of the reference and scenario simulations with this LAM are described in Giorgi et al. (2004a, b).
9. Koninklijk Nederlands Meteorologisch Instituut (KNMI) uses RACMO2 (Lenderink et al. 2003), which combines the land surface characteristics and the dynamical core of the HIRLAM Numerical Weather Prediction System with the physical parameterization of the European Centre for Medium-range Weather Forecasting (ECMWF), the version used in the 40-year reanalysis (ERA40). Some modifications to mainly the land surface scheme have been applied to increase the soil hydrological reservoir and reduce the sensitivity of canopy evaporation to drought conditions.
10. The Centre National de Recherches Météorologiques (CNRM) does not use a limited area model (LAM) as the other nine RCMs. Instead, the global model ARPEGE/IFS with variable resolution is used with maximum resolution over the Mediterranean Sea (Gibelin and Déqué 2003). However, as its resolution over Europe is the same as the other RCMs, it can be considered as a LAM with full two way nesting in a global lower resolution version of ARPEGE/IFS.

The SST anomaly produced by HadCM3 in summer over the Baltic Sea corresponds to a large warming shown to be exaggerate by Kjellström et al. (2005). RCAO and RACMO use SST from RCO in this region (see also Kjellström and Ruosteenoja 2007). The other RCMs driven by HadAM3H use SSTs derived from HadCM3 (Rowell 2005). CNRM model uses an independent set of SST derived from a low resolution coupled version of ARPEGE/IFS.

2.2 Experimental design and data preparation

Only two GHG concentration scenarios from IPCC-SRES have been used in PRUDENCE, namely A2 and B2. If we except the special case of CNRM simulations mentioned above, two AGCMs have been used to provide RCMs with lateral forcings. HadAM3H (Hudson and Jones 2000a) is a GCM developed by the HC which uses the same physics as the corresponding RCM (HadRM3H). Its horizontal resolution is 140 km in the mid-latitudes (with grid spacing of 145 latitudes by 192 longitudes). ECHAM4/OPYC3 is an AOGCM developed by MPI (Roeckner et al. 1999). Its horizontal resolution is about 300 km in the

Table 1 Experiments available in PRUDENCE: number of members for each RCM (column) and combination of GHG concentration and driving GCM (row)

Experiments available in PRUDENCE										
	CNRM	DMI	ETHZ	GKSS	HC	ICTP	KNMI	MPI	SMHI	UCM
A2+HadAM3H		3	1	1	3	1	1	1	1	1
A2+ECHAM4		1							1	
A2+ARPEGE3	1									
B2+HadAM3H					1	1			1	1
B2+ECHAM4		1							1	
B2+ARPEGE3	3									

atmosphere (T42 spectral truncation). Some PRUDENCE participants have run their 30-year simulations three times, using the same RCM and the same GHG concentration scenario, but different runs with the same GCM. More details on experimental design of PRUDENCE experiments and model performances are given in Jacob et al. (2007).

Table 1 summarizes the simulations available in the PRUDENCE database we have used in this study. We have thus 25 experiments at our disposal out of 180, which were possible if Table 1 had been full. The 25 scenario simulations, plus the 18 corresponding control simulations, represent however a large amount of computation resources.

In this study, the seasonal mean responses are calculated as the difference between the mean 2071–2100 and 1961–1990 for each grid point of a common grid (0.5°×0.5°) covering the domain common to all RCMs. Therefore all results about response and uncertainty could be displayed on maps over Europe. In order to present synthetic results, we aggregate the grid points in eight boxes with relatively homogeneous climate, at least at the horizontal resolution of the RCMs. These sub-domains are described in JH Christensen and OB Christensen (2007): British Isles (BI), Iberian Peninsula (IP), France (FR), Mid-Europe (ME), Scandinavia (SC), Alps (AL), Mediterranean (MD), East-Europe (EA). The sea points, as well as the land points not covered by all RCMs, are excluded in the tables. In the figures, as grid points are considered individually, only available RCMs are used for a given grid point so that the whole European domain can be displayed. This explains the differences between the results in Scandinavian box (two RCMs do not extend North of 60°N) and the maps over Scandinavia.

3 Variance decomposition

3.1 Materials and methods

Let X be the climate response (i.e. the difference between the 2071–2100 and the 1961–1990 seasonal averages) of a field averaged over an area, e.g. DJF temperature over East-Europe. In fact, we can consider X_{ijkl} where:

- i=1–10 according to the RCM (R)
- j=1–2 according to the scenario (S)
- k=1–3 according to the driving GCM (G)
- l=1–3 according to the member of the ensemble (M)

Using a dot to represent the average with respect to the index it is substituted for, one can decompose:

$$X_{ijkl} = X_{....} + (X_{i...} - X_{...}) + \left(X_{j..} - X_{....}\right) + (X_{..k.} - X_{....}) + (X_{...l} - X_{....}) + \left(X_{ij..} - X_{i...} - X_{j..} + X_{....}\right) + \text{etc}\ldots \quad (1)$$

The full formula would take several lines and can be explained, if not developed, in statistics textbooks (Kendall et al. 1977) and in von Storch and Zwiers (1999). If we consider the variance of X, i.e. the average of $(X_{ijkl} - X_{....})^2$, it appears that the terms between parentheses in Eq. 1 are orthogonal, so that the variance V can be split into positive contributions as:

$$V = R + S + G + M + \text{RS} + \text{RG} + \text{RM} + \text{SG} + \text{SM} + \text{GM} + \text{RSG} + \text{RSM} + \text{RGM} + \text{SGM} + \text{RSGM} \quad (2)$$

with, for example:

$$R = {}^{1}_{10} \sum_{i=1}^{10} (X_{i...} - X_{....})^2 \text{ and } \text{RS} = {}^{1}_{20} \sum_{i=1}^{10} \sum_{j=1}^{2} \left(X_{ij..} - X_{i...} - X_{j..} + X_{....}\right)^2 \quad (3)$$

R is the individual part of variance due to the RCM after having averaged all other indices (scenario, GCM and member). RS is slightly more difficult to interpret: if the responses are first averaged over the GCMs and the members (indices k and l), the variance of the means is the not the sum of the individual parts R and S, but the sum $R + S + \text{RS}$.

If the variance with respect to index i is calculated for each combination of *(j,k,l)* and then averaged with respect to *(j,k,l)*, one obtains the full part of variance due to the RCM:

$$V(R) = R + \text{RS} + \text{RG} + \text{RM} + \text{RSG} + \text{RSM} + \text{RGM} + \text{RSGM} \quad (4)$$

The terms of Eq. 2 can be explained as percentages of the variance. Due to Eq. 4, the total variance V is not the sum of the four terms *V(R)*, *V(S)*, *V(G)*, and *V(M)*, as they include interaction terms like RS or RGM. But the magnitude of the four terms indicates the role of each source in the full uncertainty.

With an additional assumption that each year is an independent realization of a given climate, one could calculate the variance due to sampling with more accuracy, as in Ferro (2004), but this term will be shown to have the smallest contribution to uncertainty. So we use here only the variability of the 30-year means. One could also combine for some models the three reference simulations with the three climate scenario runs to get nine responses instead of three, but then the assumption of independence of the samples would not be satisfied.

3.2 Missing data reconstruction

Calculating the 15 terms in Eq. 2 for each variable X and each box would be a simple exercise if Table 1 did not have holes. If each term in Eq. 2 is calculated with the few data available, the algebraic properties are no longer satisfied, and the total variance V cannot be written as a sum. In addition, this way of estimating leads to biases. For example, the average of member 1 over the RCMs, the scenarios and the GCMs does not involve the same RCMs as the average of members 2 or 3. Moreover, the proportion of A2/B2

Table 2 Root mean square difference (averaged over Europe) between the reconstructed response of SMHI simulation with A2 scenario and HadAM3H forcing on the one side and, on the other side: the actual response (D1), the response with B2 scenario and HadAM3H forcing (D2), the response with A2 scenario and ECHAM4 forcing (D3), the response of HadRM3 with A2 scenario and HadAM3H forcing (D4)

Root mean square difference				
	D1	D2	D3	D4
DJF temperature (K)	0.45	1.12	1.72	0.75
JJA temperature (K)	0.44	1.53	1.71	1.19
DJF precipitation (mm/day)	0.18	0.23	0.33	0.25
JJA precipitation (mm/day)	0.15	0.16	0.16	0.21

scenarios is not the same for member 1 as for members 2 or 3. As a consequence, the variance of the sample based on mean members 1, 2 and 3, does not fairly measure the effect of interannual variability.

A solution would be to fill the empty cells corresponding to holes in Table 1 with statistical techniques in missing data reconstruction, like principal component analysis. Here we have many missing data, so this method can produce strange artifacts. The method chosen consists of reconstructing the missing data so that the full interaction term in Eq. 4 (RSGM) is minimum. The method is easy to understand in the case of two factors, e.g. RCM and scenario. Let us assume that with a set of RCMs, the mean A2 response is 3 K and the mean B2 response is 2 K. If we have a new RCM with an A2 response of 3.5 K, and no B2 simulation available, a simple guess for the B2 response consists of applying the 1 K difference between A2 and B2 to the new RCM, which yields a 2.5 K response for B2. This is equivalent to assuming that the effect of RCM and scenario are additive. Considering that the contribution of model n and scenario 2 to RS is zero is equivalent to solving:

$$X_{n2} - X_{.2} - X_{n.} + X_{..} = 0 \tag{5}$$

which gives for model n and scenario B2 a guess X_{n2} of 2.5 K. Note that the assumption that the effects are multiplicative (3.5×2 K/3 K) leads to a different guess (2.33 K), but this approach is more difficult to generalize in a context of analysis of variance.

The case of four factors is more complex, but the principle is the same: assume additivity of the effects by neglecting the contributions to RSGM. Details on the full procedure are given in Appendix A.

The four-dimensional array X is thus completed by this procedure. In order to check that the above procedure does not produce unrealistic data, a simple verification has been performed. We restarted the full procedure, removing the A2 experiment with SMHI model and HadAM3H forcing from the data, and reconstructed it. Then, we calculated the root mean square difference (RMSD) over Europe between the actual and the reconstructed field. It is clear that the result cannot fit perfectly, otherwise we could save many computation hours. Table 2 compares this RMSD (D1) with RMSDs between the reconstructed field and other responses: the B2/HadAM3H experiment (D2), the A2/ECHAM4 experiment (D3). The reconstruction error (D1) is also compared with the RMSD between SMHI model and HadRM3 (D4). Considering the values in Table 2, it appears, in particular for temperature, that the reconstructed response is closer to the original one than to responses obtained from experiments run under different conditions.

Table 3 Percentage of variance explained by the 15 terms in the decomposition of temperature spread over the 8 boxes in DJF (Eq. 2)

Box	R	S	G	M	RS	RG	RM	SG	SM	GM	RSG	RSM	RGM	SGM	RSGM
BI	7	10	71	1	2	3	1	1	2	1	1	0	0	1	0
IP	13	21	54	1	3	3	1	2	1	1	1	0	0	0	0
FR	10	11	65	0	2	4	1	2	2	1	1	0	0	1	0
ME	12	12	55	1	3	4	1	3	4	2	1	0	0	1	0
SC	49	8	31	3	0	2	1	2	1	3	0	0	0	0	0
AL	13	15	53	3	2	3	0	3	3	1	1	0	0	1	0
MD	11	22	48	3	3	3	0	5	2	1	1	0	0	1	0
EA	15	15	47	4	3	4	1	4	4	2	1	0	0	1	0

3.3 Decomposition

Once the missing data has been reconstructed, the 15 right-hand terms of Eq. 2 are computed for each sub-domain and each field. They are multiplied by 100 and divided by the total variance, in order to appear as percent contributions. One should keep in mind that each term of the decomposition, named fraction of the total variance, is a biased estimate of variance. It is an average of squared departures to a mean. An unbiased estimate of the variance should be divided by $n-1$, but in Eq. 2 the contributions must be divided by n for algebraic reasons. In the case of the scenario ($n=2$) the contribution is only one half of the unbiased estimate of the variance. Thus, in the present study, the contribution of the scenarios, GCMs, and interannual variability to the total variance underestimates the actual variability of their effects.

Table 3 shows the 15 percentages for the eight sub-domains, for 2 m temperature in DJF. One can see that the interaction terms are generally below 5%. This is just a consequence of the reconstruction method. As we ignore much of the interaction between the different uncertainty sources because the array X_{ijkl} has many empty values, we decided to attribute arbitrarily the maximum variance to the individual contributions R, S, G and M. This variance attribution should not have a too detrimental effect on the aggregated contributions $V(R)$, $V(S)$, $V(G)$ and $V(M)$. Indeed the conclusions of Section 3.4 remain in agreement with earlier studies based on sub-arrays of X_{ijkl} without data reconstruction (Ferro 2004; Rowell 2006; Déqué 2004). The goal of our analysis is to discriminate the four sources, rather than

Table 4 Percentage of the total variance explained by RCM ($V(R)$), scenario ($V(S)$), GCM ($V(G)$), and ensemble member ($V(M)$) in the decomposition of temperature spread over the 8 boxes and the whole European domain (EU) in DJF (Eq. 4). The last column indicates the standard deviation (K)

Box	V(R)	V(S)	V(G)	V(M)	StD
BI	14	15	78	6	0.7
IP	21	27	61	3	0.8
FR	18	19	74	5	0.9
ME	21	24	66	10	1.0
SC	53	12	38	8	1.1
AL	21	25	63	8	1.0
MD	19	34	59	7	0.7
EA	23	27	59	12	1.0
EU	27	23	58	8	0.9

Table 5 As Table 4 for JJA temperature(K)

Box	V(R)	V(S)	V(G)	V(M)	StD
BI	14	23	72	4	0.7
IP	13	48	47	3	1.2
FR	17	41	53	3	1.6
ME	25	39	51	3	1.4
SC	56	28	28	5	0.8
AL	24	45	44	3	1.6
MD	23	47	40	2	1.1
EA	39	37	39	2	1.4
EU	27	41	44	3	1.2

to analyze their interactions. Analyzing the interactions will be possible when a larger set of simulations is available.

3.4 Aggregation

As mentioned above, our main interest is to know which role is played by each of the four sources of uncertainty. We thus aggregated the 15 contributions to produce *V(R)*, *V(S)*, *V(G)* and *V(M)* as explained in Eq. 4. In this case, the sum of the four percentages is greater than 100, because of the interaction terms.

Tables 4, 5, 6, and 7 indicate the four percentages. In addition, a fifth column gives the standard deviation √V. This quantity gives a measure of the uncertainty in each area. The bottom line of each table provides the percentages and standard deviation in a ninth area containing all land points of the European domain. Although the results are not spatially homogeneous, it is important to synthesize the effects of the four sources of uncertainty.

The uncertainty due to GCM is the largest out of the four, except for summer precipitation, where the choice of the RCM is the major source. This behavior can be explained by the fact that JJA precipitation is due to local processes (convection) that are marginally driven by the lateral conditions, whereas the other variables are more dependent on the general circulation.

There are also geographical differences. In the Scandinavian area, the RCM dominates. This result should be considered with caution, as the SST in the Baltic Sea is not the same for all RCMs (see Section 2.1). Although the sea points have been removed from the analysis, this inhomogeneity in the sample produces a local spread (Kjellström and Ruosteenoja 2007). In Mid-Europe the GCM uncertainty is the largest one whatever the season or the field. This area is far from the boundaries, and should less depend on the

Table 6 As Table 4 for DJF precipitation (mm/day)

Box	V(R)	V(S)	V(G)	V(M)	StD
BI	39	18	63	11	0.33
IP	28	31	30	53	0.16
FR	53	33	44	10	0.30
ME	31	12	65	8	0.27
SC	32	10	65	7	0.26
AL	49	39	54	8	0.25
MD	44	29	42	13	0.17
EA	60	9	36	12	0.16
EU	41	20	54	13	0.22

Table 7 As Table 4 for JJA precipitation (mm/day)

Box	V(R)	V(S)	V(G)	V(M)	StD
BI	52	18	36	15	0.22
IP	38	25	44	6	0.14
FR	32	44	33	12	0.21
ME	27	36	50	5	0.34
SC	81	8	16	4	0.31
AL	28	44	40	12	0.41
MD	59	14	34	7	0.16
EA	58	21	32	4	0.29
EU	50	25	34	7	0.27

driving GCM, in particular in summer. But this area is still under oceanic influence for its northern half, and changes in the general circulation produce regional changes. The uncertainty due to sampling is marginal, except for winter precipitation over Iberian peninsula. However, the variance over this region is four times less than the one over the British Isles and the climate change response is weak.

The uncertainty about the choice of the scenario (A2 versus B2) is maximum for summer temperature in the southern half of Europe. The Mediterranean summer drying and warming is significantly more intense under the A2 hypothesis. Note that this uncertainty would have been larger if we had included B1 and A1FI IPCC-SRES scenarios in PRUDENCE.

4 Response intervals

4.1 Simple method

In Section 3, we have used the variance approach to evaluate the respective importance of four sources of uncertainty. In the present section, we address the two sources which are most documented by the PRUDENCE experiments, namely the RCM and GCM. Sampling has been shown to be a minor source. From a modeler's point of view the scenario is an external source of uncertainty. IPCC has proposed other scenarios (e.g. A1), and PRUDENCE has chosen to concentrate on A2, and to explore B2 with a limited set of models. In order to give the same weight to each GCM, we consider in this section only the first (or the single) member of each A2 simulation: this means using the first three rows of Table 1, discarding two members of DMI and HC ensembles. A similar study could be conducted with the B2 simulations.

The manifold of models used is a good opportunity to calculate an interval for the responses in a very simple way. We have 12 simulations available. The minimum and maximum value at each grid point or for each sub-area provide the boundary of a confidence interval. For temperature, the minimum response is the mildest one, the maximum is the warmest one, since no cooling is observed in the datasets. In the case of precipitation, the minimum response may be the driest or the wettest one. Here we consider the mean response (average of the 12 values): if it is positive, the minimum response is the driest one. Otherwise, it is the wettest one. When the minimum and maximum are of opposite signs, the sign of the PRUDENCE response is considered as non-significant.

Table 8 provides the interval boundaries for the four fields and the eight subareas. The minimum and maximum in each box is not the absolute minimum and maximum in the box, but the spatial average of the grid point minimum and maximum. Otherwise, the amplitude of

Table 8 Minimum and maximum values in the eight European boxes in the various IPCC-SRES A2 scenarios for temperature in DJF and JJA (K) and precipitation in DJF and JJA (mm/day)

Box	Temp DJF		Temp JJA		Prec DJF		Prec JJA	
BI	1.4	3.5	2.1	4.4	0.26	1.48	−0.14	−1.18
IP	2.4	4.1	4.1	7.6	0.01	0.04	−0.13	−0.80
FR	2.1	4.3	3.8	8.6	0.18	1.26	−0.44	−1.15
ME	2.4	4.9	3.0	6.9	0.14	1.02	−0.07	−1.15
SC	1.9	3.5	1.6	3.3	0.18	1.07	0.05	−0.08
AL	2.6	5.0	3.9	8.4	−0.08	1.16	−0.18	−1.81
MD	2.7	4.2	3.9	6.8	−0.08	−0.36	−0.08	−0.86
EA	3.4	6.0	3.1	6.9	0.02	0.63	0.14	−0.94

the intervals would be biased by the size of the boxes. For temperature, the absolute minimum is obtained in winter over the British Isles (1.4 K), the absolute maximum is found in summer over France (8.6 K). Compared to the uncertainty about the global expected response to the A2 scenario (2.5 K according to IPCC 2001), this range 1.4–8.6 K is huge. However, this spread is not an uncertainty, as the variations according to the region and the season are consistent amongst the models (the largest responses are found in the same regions and seasons whatever the model).

In the case of precipitation, Table 8 reveals a non-significant response in winter over the Alps and in summer over Scandinavia and East-Europe. In winter precipitation decreases over the Mediterranean area and increases in the other regions. In summer, it decreases everywhere else than in Scandinavia and East-Europe.

4.2 Gaussian assumption

The above method has the merit of simplicity, but suffers from a drawback. The results depend strongly on the most and least sensitive RCMs and it is therefore subjective to any outlier in the sample. Adding more models automatically increases the amplitude of the intervals. Another method is to calculate intervals based on probability rather than extremes. One can calculate these probabilities from empirical frequencies. Here we prefer to use a parametric approach since the quantities considered here are averages over about 30 years (2,700 daily values). Even if daily precipitation does not have a Gaussian distribution, the central limit theorem indicates that averages of large samples can usually be considered as Gaussian variables. Moreover, averaging several experiments and averaging over boxes increases the Gaussian character of the mean responses. A statistics theorem indicates that if n independent samples of a population with variance V are averaged, the result A has a variance V/n. Here $n=12$. With the Gaussian assumption, a 99% confidence interval is :

$$(A - 2.6\sqrt{V/12} \quad , \quad A + 2.6\sqrt{V/12}) \tag{6}$$

A and V are calculated with the 30 experiments (3 GCMs and 10 RCMs), including reconstructed values, in order to avoid to give too much weight to the HadAM3 forcing. We used the same 12 experiments as in Section 4.1, plus the 18 reconstructed values in the empty cells of the first three rows of Table 1. Table 9 shows the boundary intervals which can be compared with Table 8. There is an important difference, however. In Table 8, the interval concerns the result of a single simulation, whereas in Table 9 it concerns the average of 12 independent simulations. The final PRUDENCE outcome being the multimodel average,

Table 9 Boundaries of the 99% confidence interval in the eight European boxes in the various IPCC-SRES A2 scenarios for temperature in DJF and JJA (K) and precipitation in DJF and JJA (mm/day)

Box	Temp DJF		Temp JJA		Prec DJF		Prec JJA	
BI	1.4	2.8	2.3	3.7	0.40	1.04	−0.21	−0.78
IP	2.5	3.7	4.2	6.4	0.00	0.10	−0.23	−0.57
FR	2.1	3.6	3.8	6.7	0.20	0.77	−0.52	−0.93
ME	2.4	4.1	2.9	5.5	0.14	0.68	−0.18	−0.84
SC	2.0	3.0	1.7	2.8	0.26	0.75	−0.03	−0.11
AL	2.7	4.3	3.9	6.7	0.01	0.69	−0.27	−1.21
MD	2.8	3.9	3.9	5.9	−0.08	−0.31	−0.09	−0.48
EA	3.4	5.1	3.3	5.8	0.09	0.43	−0.02	−0.63

Table 9 is a more suitable approach toward confidence in the results. The intervals are narrower, and there are no cases with the zero value between the boundaries, which indicates that the sign of all responses is statistically significant. In the case of winter over the Alps and summer over Scandinavia and East-Europe, for which Table 8 shows no unanimity about the sign of the response, the lower boundary is close to zero. This is also the case with winter precipitation over Iberian Peninsula. This case presents a tiny response to climate change: this explains why sampling uncertainty is a large source of uncertainty, compared to the other three (see Section 3.4).

The results of Table 9 can be presented as maps, by plotting the upper and lower boundaries at each grid point (with consideration of the sign of the average in the case of precipitation as in Section 4.1). Figures 1, 2, 3, and 4 presents the pairs of maps for the four fields. In the case of temperature, as the variance is more spatially homogeneous than the mean, the lower and upper boundaries show similar structures: West-East gradient in winter, North–South gradient in summer. The winter gradient is mostly explained by the role of snow cover in cooling down the surface through snow albedo and snow emissivity feedbacks. In a

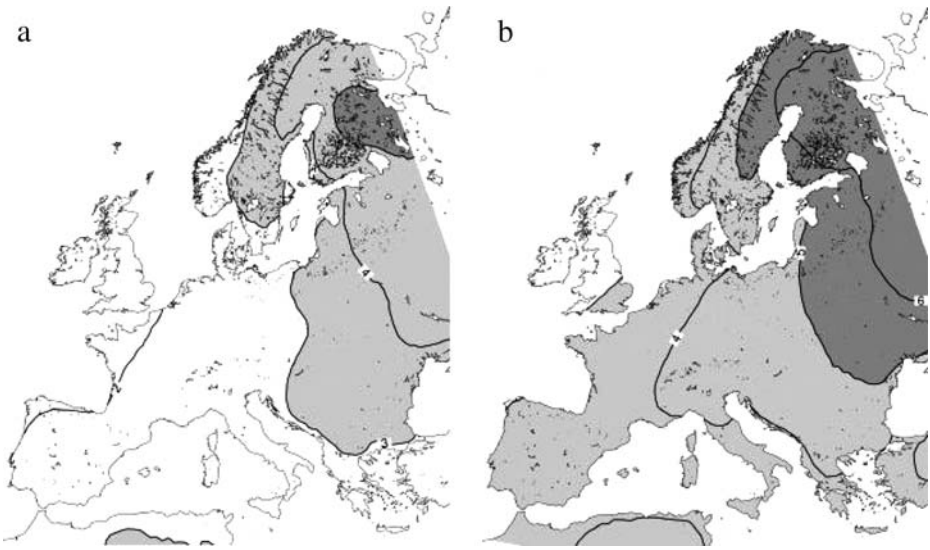

Fig. 1 Lower (**a**) and upper (**b**) boundaries of the 99% interval for the mean response to scenario A2: DJF temperature; contour interval 1 K, light shading above 3 K, dense shading above 5 K

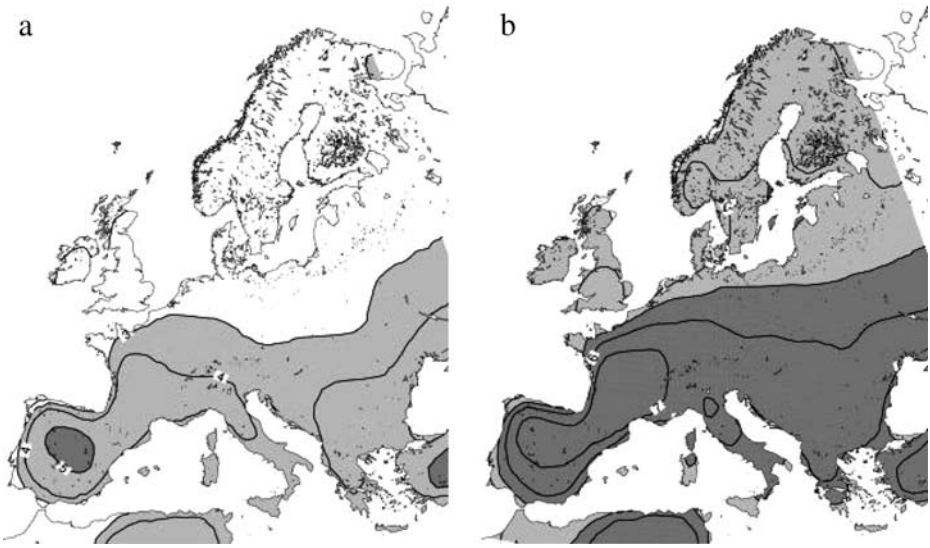

Fig. 2 As Fig. 1 for JJA temperature

warmer climate, the winter snowline is pushed eastwards and northwards. The summer gradient is partly explained by the fact that southern Europe (except the Alps) has less soil moisture available: evapotranspiration cannot as efficiently counteract the energy absorbed by the land surface from solar radiation. In the A2 climate scenario, the soils are dry in this part (no precipitation increase to compensate potential evaporation increase), and temperature raise is less tempered by evapotranspiration than in the northern part.

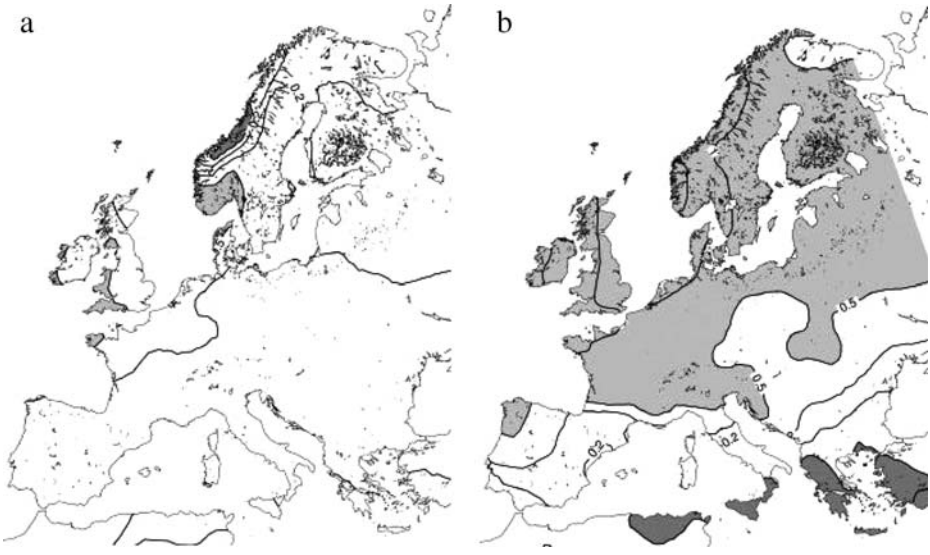

Fig. 3 As Fig. 1 for DJF precipitation; contours ±0.2, ±0.5, ±1, ±2 mm/day, light shading above +0.5 mm/day, dense shading below −0.5 mm/day

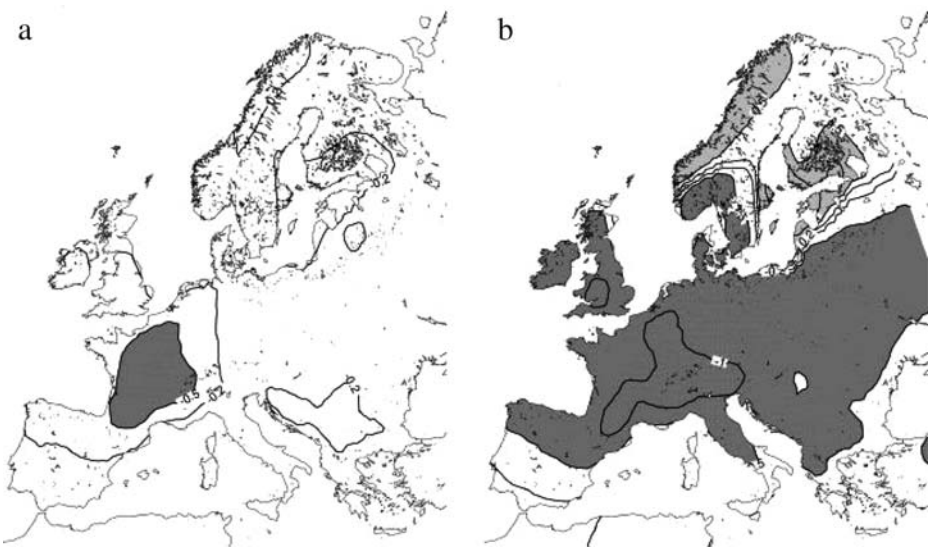

Fig. 4 As Fig. 3 for JJA precipitation

Precipitation maps have more complex structures, and the lower boundaries exhibit responses between −0.2 and 0.2 mm/day. Along the north-western coasts of Norway, the lower boundary is negative for DJF precipitation, whereas the upper boundary is positive: the mean response is not significant there. This feature comes from large differences between the driving GCMs (Räisänen et al. 2004). Along the Baltic Sea coasts in JJA, there is also a change in sign between the minimum and maximum values. As mentioned above, the fact that the RCMs do not use the same SST forcing in this region contributes to a large spread in the area.

5 Summary and conclusions

The PRUDENCE project has produced an ensemble of simulations involving different scenarios, different RCMs and different GCMs. Some runs have been repeated three times to take into account the internal variability. The seasonal multi-year means of this dataset have been exploited to investigate the uncertainty about the mean result, evaluated through the spread of the mean responses over sub-areas of the European domain.

The first question was the respective role of the various sources of uncertainty. As we have only a few of all possible combinations of scenarios, RCMs and GCMs at our disposal, artificial responses have been calculated to avoid favoring the A2/HadAM3 combination in calculating the variances. Then the variance has been partitioned and aggregated into four contributions, corresponding to the RCM, the scenario, the GCM, and the member of the sample. The uncertainty introduced by the choice of the driving GCM is generally larger than the other three sources. For summer precipitation the choice of the RCM is a source of uncertainty which has the same magnitude as the choice of the GCM, if we discard the case of Scandinavia in which RCM uncertainty includes the use of different SSTs. The uncertainty arising from the choice of the scenario is maximum for summer temperature in the southern half of Europe where the largest response is obtained. In

PRUDENCE, only A2 and B2 have been considered, which corresponds, in terms of GHG concentration spread, of 50% of the range of the nine IPCC-SRES scenarios. The uncertainty due to sampling is marginal, except for winter precipitation over the Iberian peninsula where the mean response is negligible.

These results show that, if we want to design an efficient approach toward uncertainty based on several models, the number of GCMs involved should at least equilibrate the number of RCMs. The role of GCMs is possibly underestimated here, as IPCC results suggest that HadCM3 and ECHAM4 do not span the full range of uncertainty. It is also necessary to explore other scenarios than A2 and B2 in the case of southern Europe summer warming.

The second question addressed by this study was the evaluation of a minimum and a maximum response. Intervals are in some case a useful approach toward uncertainty. It is shown that the temperature amplitude about the PRUDENCE multimodel A2 response is between 1 and 3 K according to the region and season. The precipitation intervals are rather broad for some areas: (0.4–1.0 mm/day) for British Isles in winter. But the response is always significantly different from zero. Using several models reveals the amplitude of the uncertainties, but also helps to reduce them. One must keep in mind that, in our approach, uncertainty is not a measure of forecast quality. We have no means, by such techniques, to claim that the future climate will lie between the boundaries of the intervals. Other sources of uncertainty (reliability of SRES scenarios, ability of a GCM or RCM to provide the exact response to a forcing we have never observed before, other unexpected phenomena like volcano eruptions, ...) cannot be objectively deduced from numerical simulations. We simply state that we have explored the possibility of the state of the art models. So at present the most comprehensive estimate of future regional climate change over Europe are as documented in this work.

Acknowledgments This work was supported by the European Commission Programme Energy, Environment and Sustainable Development under contract EVK2-2001-00156 (PRUDENCE). The French contribution was partly supported by the GICC-IMFREX contract of the Department of Environment (MEDD). D.P.Rowell's contribution has been partly supported by Department of Environment, Food and Rural Affairs (contract PECD 7/12/37). The authors are grateful to Dr O. B. Christensen (DMI) for preparing the database with regional scenarios and to C.A.T. Ferro (Univ. Reading) for his helpful comments on analysis of variance. The authors are also indebted to two anonymous referees for their suggestions.

Data reconstruction algorithm

The aim of this method is to generalize the rule of thumb mentioned in Section 3.2 which described the case of a two dimensional array. We want to complete a four dimensional array with many missing data. The data to be reconstructed are sub-domain averages (Section 3) or grid point values (Section 4.2). The completion algorithm works in six steps:

- Step 1: we calculate the full average $X_{....}$ with available data.
- Step 2: we calculate the triple averages like $X_{i...}$ with available data, which is straightforward, since for each RCM we have at least one simulation. Same operation for $X_{.j..}$, $X_{..k.}$ and $X_{...l}$.
- Step 3: we calculate the double averages like $X_{ij..}$. Here some pairs cannot be calculated because of missing data, for example there is no ETHZ experiment with B2 scenario. We use the principle of minimizing the interaction terms. For example the *RS* term is the sum of the $\left(X_{ij..} - X_{i...} - X_{.j..} + X_{....}\right)^2$ over i and j; we simply set

$X_{ij..} = X_{i...} + X_{.j..} - X_{....}$ when this term is missing. This is another formulation of Eq. 5. Same operations for $X_{i.k.}$, $X_{i..l}$, $X_{.jk.}$, $X_{.j.l}$ and $X_{..kl}$.

- Step 4: we calculate the simple averages like $X_{ijk.}$ with available data. Those which cannot be calculated are deduced from the full, triple and double averages as in Step 3. Same operations for $X_{ij.l}$, $X_{i.kl}$ and $X_{.jkl}$.
- Step 5: RSGM term is a sum of squared linear combinations involving an X_{ijkl} and some averages. At this stage all averages are available (simple, double, triple and full averages), as a first guest, from the previous steps. Those X_{ijkl} which are missing are calculated so that the corresponding linear combination is zero.
- Step 6: in fact the missing X_{ijkl} should have been involved also in the averages, but they have not been taken into account in the previous steps. A method would be to solve a system of implicit equations. As the system to be solved is linear, an iterative method is easier to implement and efficient. Step 5 is repeated 10 times. The right-hand side averages (simple, double, triple and full averages) in the equations are calculated with the solutions from the previous iteration. Only the missing X_{ijkl} are updated. After 10 iterations, the increment of all missing X_{ijkl} is less than 0.1%.

References

Aldrian E, Dümenil Gates L, Jacob D, Podzun R, Gunawan D (2004) Long term simulation of the Indonesian rainfall with the MPI Regional Model. Clim Dyn 22:795–814

Arribas A, Gallardo C, Gaertner MA, Castro M (2003) Sensitivity of Iberian Peninsula climate to land degradation. Clim Dyn 20:477–489

Castro M, Fernández C, Gaertner MA (1993) Description of a meso-scale atmospheric numerical model. In: JI Díaz, JL Lions (eds) Mathematics, climate and environment, Masson

Christensen JH, Christensen OB (2003) Climate modelling: severe summertime flooding in Europe. Nature 421:805–806

Christensen OB, Christensen JH (2004) Intensification of extreme European summer precipitation in a warmer climate. Glob Planet Change 44:107–117

Christensen JH, Christensen OB (2007) A summary of the PRUDENCE model projections of changes in European climate by the end of this century. Clim Change, doi:10.1007/s10584-006-9210-7 (this issue)

Christensen JH, van Meijgaard E (1992) On the construction of a regional atmospheric climate model, DMI Technical Report 92–14. Available from DMI, Lyngbyvej 100, Copenhagen Ø

Christensen JH, Christensen OB, Lopez P, van Meijgaard E, Botzet M (1996) The HIRHAM4 regional atmospheric climate model, DMI Technical Report 96–4. Available from DMI, Lyngbyvej 100, Copenhagen Ø

Christensen OB, Christensen JH, Machenhauer B, Botzet M (1998) Very high-resolution regional climate simulations over Scandinavia – present climate. J Climate 11:3204–3229

Christensen JH, Christensen OB, Schultz JP (2001) High resolution physiographic data set for HIRHAM4: An application to a 50 km horizontal resolution domain covering Europe, DMI Technical Report 01–15. Available from DMI, Lyngbyvej 100, Copenhagen Ø

Christensen JH, CarterTR, Giorgi F (2002) PRUDENCE employs new methods to assess European climate change. EOS 83:147

Crossley JF, Polcher J, Cox PM, Gedney N, Planton S (2000) Uncertainties linked to land-surface processes in climate change simulations. Clim Dyn 16:949–961

Déqué M (2004) Uncertainties in PRUDENCE simulations: Global high resolution models, PRUDENCE Technical Report. Available at Météo-France, 42 Avenue Coriolis, 31057 Toulouse, France, pp 58

Döscher R, Willén U, Jones CG, Rutgersson A, Meier H, Hansson E, Graham M (2002) The development of the coupled regional ocean-atmosphere model RCAO. Boreal Environ Res 7:183–192

Ferro CAT (2004) Attributing variation in a regional climate change modelling experiment, PRUDENCE Technical Report. Available at Dept. of Meteorology, University of Reading, Earley Gate, PO Box 243, Reading RG6 6BB, UK, 21 pp

Frei C, Christensen JH, Déqué M, Jacob D, Jones RG, Vidale PL (2003) Daily precipitation statistics in regional climate models: Evaluation and intercomparison for the European Alps. J Geophys Res 108 (D3):4124 doi:101029/2002JD002287

Gaertner MA, Christensen OB, Prego JA, Polcher J, Gallardo C, Castro M (2001) The impact of deforestation on the hydrological cycle in the western Mediterranean: an ensemble study with two regional climate models. Clim Dyn 17:857–873

Gallardo C, Arribas A, Prego JA, Gaertner MA, Castro M (2001) Multi-year simulations with a high resolution regional climate model over the Iberian Peninsula: Current climate and 2xCO2 scenario. Quart J Roy Meteor Soc 127:1659–1682

Gibelin AL, Déqué M (2003) Anthropogenic climate change over the Mediterranean region simulated by a global variable resolution model. Clim Dyn 20:327–339

Giorgi F, Francisco R (2000) Uncertainties in regional climate change prediction: a regional analysis of ensemble simulations with the HADCM2 coupled AOGCM. Clim Dyn 16:169–182

Giorgi F, Marinucci MR, Bates GT (1993a) Development of a second generation regional climate model (REGCM2). Part I: Boundary layer and radiative transfer processes. Mon Weather Rev 121:2794–2813

Giorgi F, Marinucci MR, Bates GT, DeCanio G (1993b) Development of a second generation regional climate model (REGCM2). Part II: Convective processes and assimilation of lateral boundary conditions. Mon Weather Rev 21:2814–2832

Giorgi F, Huang Y, Nishizawa K, Fu C (1999) A seasonal cycle simulation over eastern Asia and its sensitivity to radiative transfer and surface processes. J Geophys Res 104:6403–6423

Giorgi F, Bi X, Pal JS (2004a) Means, trends and interannual variability in a regional climate change experiment over Europe. Part I: present day climate (1961–1990). Clim Dyn 22:733–756

Giorgi F, Bi X, Pal JS (2004b) Means, trends and interannual variability in a regional climate change experiment over Europe. Part II: future climate scenarios (2071–2100). Clim Dyn 23:839–858

Hagemann S, Botzet M, Dümenil L, Machenhauer B (1999) Derivation of global GCM boundary conditions from 1 km land use satellite data, MPI Report, Max-Planck Institut für Meteorologie 289

Heck P, Lüthi D, Wernli H, Schär C (2001) Climate impacts of European-scale anthropogenic vegetation changes: a study with a regional climate model. J Geophys Res-Atmos 106(D8):7817–7835

Hennemuth B, Rutgersson A, Bumke K, Clemens M, Omstedt A, Jacob D, Smedman AS (2003) Net precipitation over the Baltic Sea for one year using models and data-based methods. Tellus 55A:352–367

Hudson DA, Jones RG (2002a) Simulations of present-day and future climate over southern Africa using HadAM3H, Hadley Centre Technical Note no 38, Met Office, Exeter, UK

Hudson DA, Jones RG (2002b) Regional climate model simulations of present-day and future climates of southern Africa, Hadley Centre Technical Note no 39, Met Office, Exeter, UK

IPCC (2001) Climate change. The scientific basis. The Edinburgh Building Shaftesbury Road, Cambridge CB2 2RU England pp 881

Jacob D (2001) A note to the simulation of the annual and inter-annual variability of the water budget over the Baltic Sea drainage basin. Meteorol Atmos Phys 77:61–73

Jacob D, Bärring L, Christensen OB, Christensen JH, Castro M, Déqué M, Giorgi F, Hagemann S, Hirschi M, Jones R, Kjellström E, Lenderink G, Rockel B, Sanchez E, Schär C, Seneviratne, SI, Somot S, van Ulden A, van den Hurk B (2007) An inter-comparison of regional climate models for Europe: model performance in present-day climate. Clim Change, doi:10.1007/s10584-006-9213-4 (this issue)

Jones CG, Ullerstig A, Willén U, Hansson U (2004) The Rossby Centre regional atmospheric climate model (RCA). Part I: model climatology and performance characteristics for present climate over Europe. Ambio 33(4–5):199–210

Jones RG, Murphy JM, Hassell DC, Woodage MJ (2005) A high resolution atmospheric GCM for the generation of regional climate scenarios. Hadley Centre Technical Note 63, Met Office, Exeter, UK

Kendall M, Stuart A, Ord JK (1977) The advanced theory of statistics. Vol 3: design and analysis, and time series, 4th edition, Charles Griffin and Co Ltd, 780 pp

Kjellström E, Ruosteenoja K (2007) Present-day and future precipitation in the Baltic Sea region as simulated in a suite of regional climate models. Clim Change, doi:10.1007/s10584-006-9219-y (this issue)

Kjellström E, Döscher R, Meier HEM (2005) Atmospheric response to different sea surface temperatures in the Baltic Sea: coupled versus uncoupled regional climate model experiments. Nordic Hydrology 36:397–409

Lehmann A, Lorenz P, Jacob D (2004) Exceptional Baltic Sea inflow events in 2002–2003. Geophysical Research Letters, 2004GL020830

Lenderink G, van den Hurk B, van Meijgaard E, van Ulden A, Cuijpers H (2003) Simulation of present-day climate in RACMO2: first results and model developments, KNMI Technical Report 252, 24 pp

Meier HEM, Döscher R, Faxén T (2003) A multiprocessor coupled ice-ocean model for the Baltic Sea. Application to the salt inflow. J Geophys Res 108(C8):3273

Pal JS, Small EE, Eltahir EAB (2000) Simulation of regional – scale water and energy budgets: representation of subgrid cloud and precipitation processes within RegCM. J Geophys Res 105:29579–29594
Räisänen J, Hansson U, Ullerstig A, Döscher R, Graham LP, Jones C, Meier HEM, Samuelsson P, Willén U (2004) European climate in the late twenty-first century: regional simulations with two driving global models and two forcing scenarios. Clim Dyn 22:13–31
Roeckner E, Bengtsson L, Feichter J, Lelieveld J, Rodhe H (1999) Transient climate change simulations with a coupled atmosphere-ocean GCM including the tropospheric sulfur cycle. J Climate 12:3004–3032
Rowell DP (2005) A scenario of European climate change for the late 21st century: seasonal means and interannual variability. Clim Dyn 25:837–849
Rowell DP (2006) A demonstration of the uncertainty in projections of the UK climate change resulting from regional model formulation. Clim Change 79:243–257
Sanchez E, Gallardo C, Gaertner MA, Arribas A, Castro A (2004) Future climate extreme events in the Mediterranean simulated by a regional climate model: a first approach. Glob Planet Change 44:163–180
Schär C, Lüthi D, Beyerle U, Heise E (1999) The soil-precipitation feedback: a process study with a regional climate model. J Climate 12:722–741
Schär C, Vidale PL, Lüthi D, Frei C, Häberli C, Liniger MA, Appenzeller C (2004) The role of increasing temperature variability in European summer heatwaves. Nature 427:332–336
Semmler T, Jacob D, Schlünzen KH, Podzun R (2004) Influence of sea ice treatment in a regional climate model on boundary layer values in the Fram Strait region. Mon Weather Rev 132:985–999
Steppeler J, Doms G, Schättler U, Bitzer HW, Gassmann A, Damrath U, Gregoric G (2003) Meso-gamma scale forecasts using the nonhydrostatic model LM. Meteorol Atmos Phys 82:75–96
Vidale PL, Lüthi D, Frei C, Seneviratne S, Schär C (2003) Predictability and uncertainty in a regional climate model. J Geophys Res 108(D18):4586, doi:10.1029/2002JD002810
Von Storch H, Zwiers FW (1999) Statistical analysis in climate research. Cambridge University Press, UK, p 484